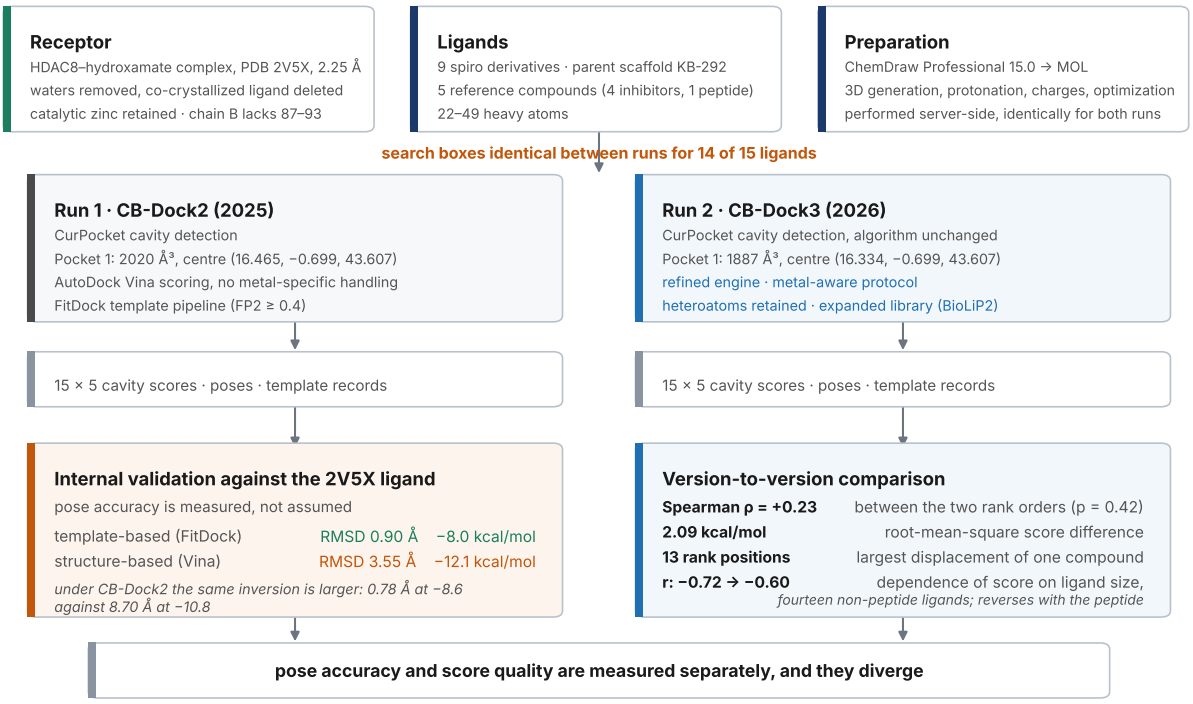
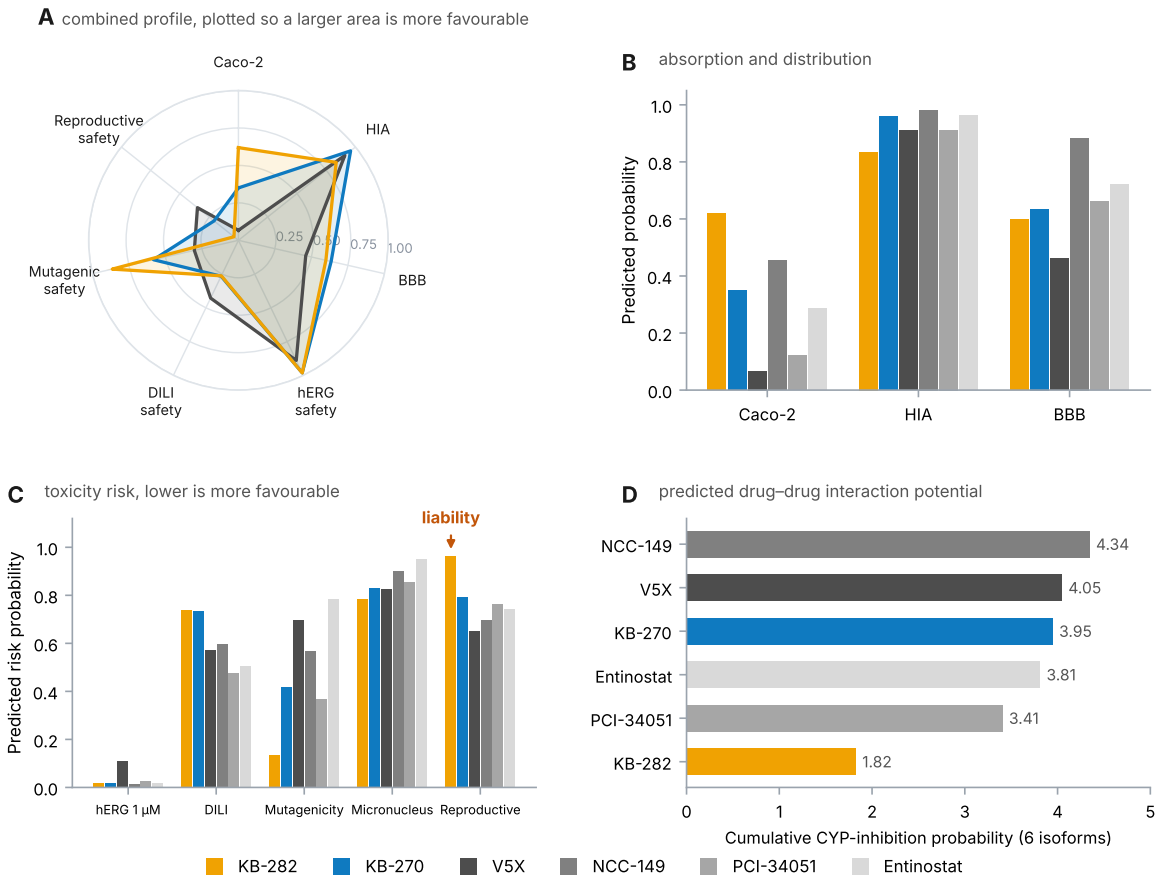


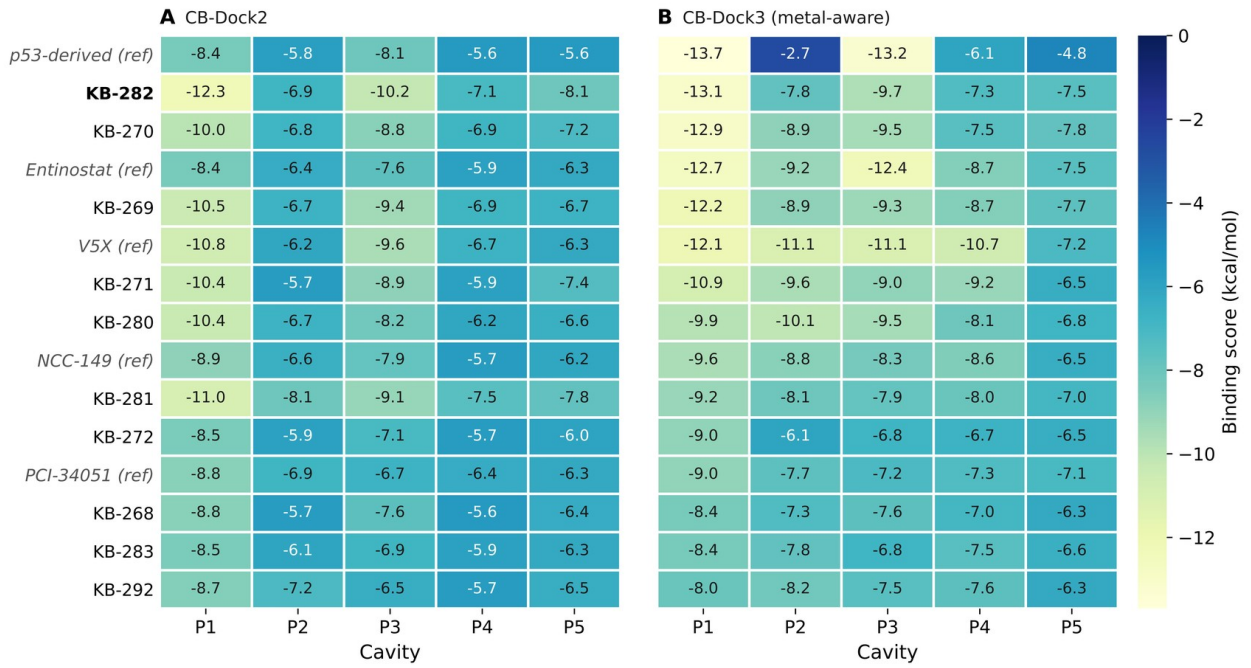
All 75 ligand–cavity runs converged. KB-272 (Pocket 1) and PCI-34051 (Pocket 3) returned a positive score on first submission and converged on resubmission of identical input; the converged values are used throughout.

Deviations are computed in place over the 46 heavy atoms in a shared coordinate frame with symmetry-corrected atom mapping. Each ligand was submitted once to each version; no replicate submissions were performed.

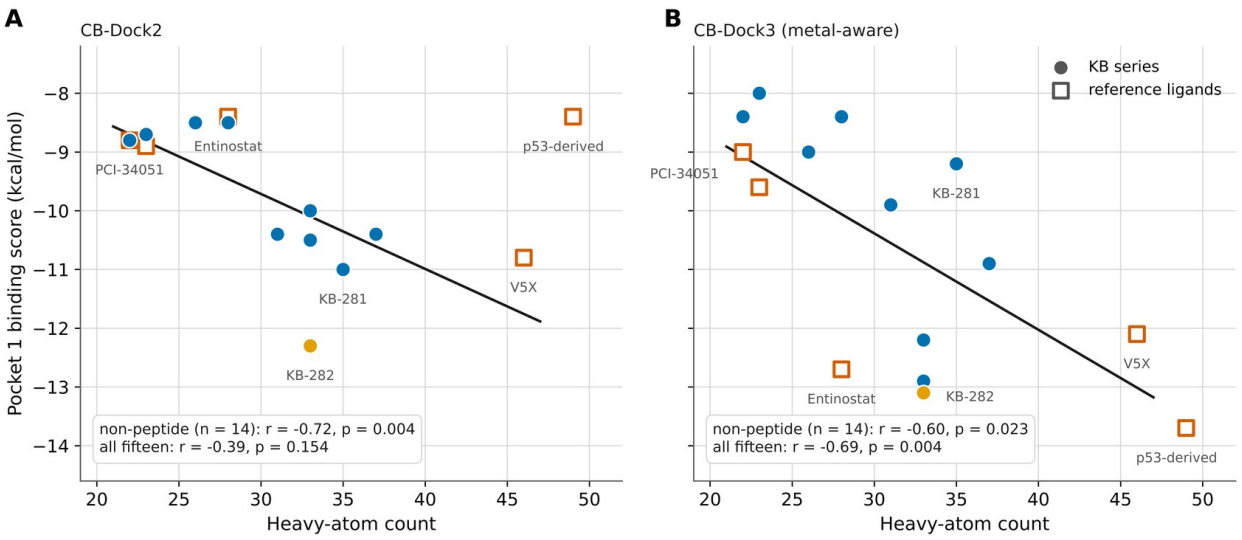
Supplementary Figure S1. Design of the two-version comparison: the shared inputs, the two docking arms and the points at which they differ, the internal pose-accuracy validation against the co-crystallized 2V5X ligand, and the version-to-version comparison. Cavity volumes and centres are those returned by CurPocket for each run. Statistics are those of Supplementary Table S13; all seventy-five ligand–cavity runs converged.



Supplementary Figure S2. Predicted ADMET profile of the compounds nominated under either protocol, set against the reference inhibitors. (A) Combined profile for KB-282, KB-270 and V5X, plotted as safety scores (1 − risk for the toxicity endpoints) so that a larger area is more favourable. (B) Absorption and distribution. (C) Toxicity risk, lower being more favourable; the arrow marks the reproductive-toxicity liability discussed under *Cytotoxicity and predicted ADMET profile*. (D) Cumulative CYP-inhibition probability summed over six isoforms. All values are admetSAR 3.0 outputs, read from Supplementary Tables S5, S7 and S8.



Supplementary Figure S3. Heat map of binding scores across the five detected HDAC8 cavities under both server versions. Panels: (A) CB-Dock2; (B) CB-Dock3. Colour encodes the score on the scale shown, pale cells denoting the more negative values and dark cells those closer to zero. Compounds are ordered by CB-Dock3 Pocket 1 score. All seventy-five runs converged after the resubmissions described under *Reproducibility of the ranking between server versions*. Data from Supplementary Tables S2 and S3.



Supplementary Figure S4. Dependence of the Pocket 1 binding score on ligand size under both server versions. Binding scores plotted against heavy-atom count for (A) CB-Dock2 and (B) CB-Dock3. Filled circles denote the spiro derivatives and the parent scaffold KB-292, with KB-282 highlighted; open squares denote the reference compounds. Solid lines are least-squares fits over the fourteen non-peptide ligands. Coefficients are given for that fit and, inset, for the full set of fifteen including the p53-derived peptide, which reverses the direction of the version-to-version change (see *Dependence of the ranking on ligand size*).

Supplementary Note 1. Abbreviations

ADMET, absorption, distribution, metabolism, excretion, and toxicity; AhR, aryl hydrocarbon receptor; APCI, atmospheric pressure chemical ionization; AR, androgen receptor; AR-LBD, androgen receptor ligand-binding domain; ARE, antioxidant response element; ATAD5, ATPase family AAA domain-containing protein 5; ATCC, American Type Culture Collection; BBB, blood–brain barrier; BCF, bioconcentration factor; BCRP, breast cancer resistance protein; BSEP, bile salt export pump; CASF, comparative assessment of scoring functions; CB-Dock2 / CB-Dock3, cavity detection-guided blind docking server, versions 2 and 3; CLMGraph, deep-learning logP prediction model; CLp, plasma clearance; CLr, renal clearance; CurPocket, protein-surface-curvature-based pocket detection algorithm; CYP, cytochrome P450; DDI, drug–drug interaction; df, degrees of freedom; DILI, drug-induced liver injury; DMEM, Dulbecco's Modified Eagle Medium; DMSO, dimethyl sulfoxide; EI-MS, electron impact mass spectrometry; ER, estrogen receptor; ER-LBD, estrogen receptor ligand-binding domain; ERRα, estrogen-related receptor alpha; FitDock, template-based fitting docking algorithm; FP2, fingerprint type 2; GR, glucocorticoid receptor; H, Kruskal–Wallis test statistic; HBA, hydrogen bond acceptors; HBD, hydrogen bond donors; HDAC, histone deacetylase; HDAC8, histone deacetylase isoform 8; HDACi, HDAC inhibitor(s); hERG, human ether-à-go-go-related gene channel; HIA, human intestinal absorption; HLM, human liver microsomal stability; IC_{50}, half-maximal inhibitory concentration; IR, infrared spectroscopy; L1 loop, loop 1 of HDAC8; LC-MS, liquid chromatography–mass spectrometry; LE, ligand efficiency; LogP, logarithm of octanol–water partition coefficient; logS, logarithm of aqueous solubility; MATE1, multidrug and toxin extrusion protein 1; MMP, mitochondrial membrane potential; MOL, MDL molfile format; MRT, mean residence time; MTT, 3-(4,5-dimethylthiazol-2-yl)-2,5-diphenyltetrazolium bromide; MW, molecular weight; NMR, nuclear magnetic resonance; nRot, number of rotatable bonds; OATP, organic anion transporting polypeptide; OCT, organic cation transporter; p53, tumour protein p53; PDB, Protein Data Bank; P-glycoprotein, P-gp efflux transporter; pKa, acid dissociation constant (logarithmic form); PPARγ, peroxisome proliferator-activated receptor gamma; PPB, plasma protein binding; r, Pearson correlation coefficient; R^2, coefficient of determination; RDKit, open-source cheminformatics toolkit; RLM, rat liver microsomal stability; RMSD, root-mean-square deviation; RPMI-1640, Roswell Park Memorial Institute medium 1640; SAR, structure–activity relationship; SD, standard deviation; SlogP, logP calculated by the RDKit algorithm; SMC3, structural maintenance of chromosomes protein 3; T½, elimination half-life; TMS, tetramethylsilane; Tox21, Toxicology in the 21st Century panel; TPSA, topological polar surface area; TR, thyroid receptor; TSA, trichostatin A; UGT, UDP-glucuronosyltransferase; VDss, steady-state volume of distribution; ZBG, zinc-binding group; ρ, Spearman rank correlation coefficient; τ, Kendall rank correlation coefficient.